# Intrazeolite Photochemistry. 22. Acid−Base Properties of Coumarin 6. Characterization in Solution, the Solid State, and Incorporated into Supramolecular Systems

**Sonia Corrent,[†] Peter Hahn,[†] Gerd Pohlers,[†] Terrence J. Connolly,[†] J. C. Scaiano,*[,†] Vicente Fornés,[‡] and Hermenegildo García*[,‡]**

*Department of Chemistry, University of Ottawa, Ottawa, Canada K1N 6N5, and Instituto de Tecnología Química, CSIC-UPV, Universidad Politécnica de Valencia, 46071 Valencia, Spain*

*Received: February 16, 1998; In Final Form: May 17, 1998*

The spectroscopic properties of the dye coumarin 6 in solution are reported. Relatively large shifts are seen in both the absorption and fluorescence spectra upon protonation. The very large Stokes shift that is seen for the dye in its solid state and as the hydrochloride salt reveals that the dye molecules are forming aggregates, which is a phenomenon that is also seen in very high concentrations of coumarin 6 in solution. The acid−base properties of coumarin 6 in heterogeneous systems such as zeolites and clays are also presented. We have found that this dye molecule is extremely sensitive to the presence of Lewis and Brønsted sites and were able to detect acidity in the faujasite zeolite NaY which is usually considered to be nonacidic. Two series of faujasite zeolites, one in which the Brønsted acidity increases and the other in which the Lewis acidity increases, were also studied. The dication of the dye was detected in both HY100 and CBV 740, the zeolites with the highest Brønsted and highest Lewis acidity, respectively, used in the present study. Due to the large shifts seen for coumarin 6 in its neutral, monocation, and dication forms, both the absorption and fluorescence spectra resulted in detection of two species of the dye in those zeolites with intermediate acidity. The ability of coumarin 6 to sense small amounts of Lewis and Brønsted sites makes it an attractive molecule to study other systems as well.

## Introduction

Zeolites are crystalline aluminosilicate structures that have been widely employed in catalytic reactions and as molecular sieves.[1] The replacement of a Si for an Al atom in the zeolite framework introduces a net negative charge. This negative charge is compensated by cations, the most common ones being alkali, alkaline earths, and protons. The cations present in the lattice can easily be exchanged by other cations using well-established techniques.[2] This results in an alteration of the chemical properties of the zeolite, namely its acid−base properties.

Zeolites may contain Lewis and Brønsted acid sites. The Lewis acid sites are due to Si or Al atom acceptors, which are considered as mild Lewis sites, as well as to extraframework Al species present in the form of $AlO^+$, $Al(OH)^{2+}$, $Al(OH)_2^+$, and oligomer polyoxoaluminates. These extraframework Al species, which are mainly produced when generating the $H^+$ form of a zeolite from the calcination of the ammonium-exchanged zeolites,[3] can enhance the acidity of the framework Brønsted site due to a polarization effect. Brønsted acidity is attributed to the bridging OH located between Si and Al atoms. The total number of Brønsted sites thus depends on the framework Si/Al ratio. Compared to a silanol group which has a p$K_a$ of 7.1 as measured for surface silanol groups on silica,[4] the acidity of the proton in the bridging hydroxyl group is much greater, which for some sites has been measured to have a negative p$K_a$. This acidity can be thought of in terms of a silanol group that undergoes Lewis acid promotion by $Al^{3+}$.

Zeolite acidity has been studied using a variety of methods,[5,6] some of which include temperature-programmed desorption of ammonia,[7−9] Raman[10−12] and IR spectroscopic studies of pyridine absorbed on zeolites,[13] solid-state NMR,[14,15] calorimetric studies,[16] and resonance Raman of a dye included within a faujasite zeolite.[17] All of the above techniques have inherent advantages and limitations associated with them. For the most part, these methods have been used in order to achieve an understanding of the types and strengths of acid sites present in proton exchanged zeolites. In those cases where alkali metal cation zeolites were employed, no Brønsted acidity could be detected.[12,17]

To further investigate the acid−base properties of a variety of zeolites, we reasoned that it may be possible to incorporate a dye molecule that can penetrate into the voids of the zeolites and monitor the resulting changes in its absorption and fluorescence spectra upon protonation. The optimal dye molecule chosen for this type of approach into the study of zeolite acidity not only needs to be sensitive to its microenvironment but also must undergo large spectral shifts upon protonation, particularly in the study of solid systems where band broadening is common. The focus of the present study is to include coumarin 6 (see below), a commercially available laser dye,[18−20] within alkali and proton exchanged zeolites and use absorption, fluorescence, and IR techniques in order to determine the relative acidity of zeolites.

Coumarin 6 was chosen because it can be readily included within faujasite zeolites and because it exhibits a large shift in its absorption $\lambda_{max}$ upon protonation: the absorption $\lambda_{max}$ in dichloromethane solution for the neutral form is at 450 nm whereas upon protonation the spectrum is red-shifted, resulting in a $\lambda_{max}$ of 520 nm for the monocation species. The IR

* To whom correspondence should be addressed.
[†] University of Ottawa.
[‡] Universidad Politécnica.

S1089-5647(98)01148-1 CCC: $15.00 
Published on Web 07/07/1998

spectrum of coumarin 6 also undergoes a large shift in its carbonyl stretching frequency upon interaction with acid sites. We illustrate the remarkable ability of this probe molecule to detect mild acidity in faujasite zeolite NaY, which cannot be readily detected using other established techniques. While not very abundant, the acid sites in NaY may play a key role in the zeolite control of chemical reactions.

The acid−base properties of coumarin 6 are also characterized in solution as well as in the solid state. The sensitivity of this dye molecule makes it feasible to study other heterogeneous systems such as clays, which this article also explores. Clays are chemically similar to zeolites but are comprised of two-dimensional layers or sheets of aluminosilicates with the charge-compensating cations located between the anionic layers, rather than the three-dimensional cages and channels that comprise zeolite structures. In contrast to zeolites, intercalation of various guest molecules within the clay minerals, especially smectites, causes their crystal layered structure to swell significantly. The relatively high cation exchange capacity (∼100 mequiv/100 g clay) and large surface area (up to 800 $m^2/g$) contribute to its notable intercalation and swelling properties.[21]

The Brønsted and Lewis acidity of clays have also been studied.[22−24] Lewis acidity within the clays arises from incompletely coordinated Al sites. Brønsted acidity arises when the cations are replaced with hydrogen ion by treatment of clay with sulfuric acid[25] or when the exchangeable cations become hydrated.

To employ coumarin 6 as described above, it is necessary to gain a detailed understanding of its solution spectroscopy, which surprisingly is not available. These aspects are also covered in this report.

## Experimental Section

The zeolite LZ-Y52 molecular sieve (NaY zeolite, Si/Al = 2.6) was obtained from Aldrich. Zeolites HY 21 and HY 100[26] were obtained according to reported procedures. HY 21 refers to a partially exchanged NaY zeolite with 21% of the Na cation replaced by H, and HY 100 refers to a completely H exchanged Y zeolite. CBV 720 (Si/Al = 15) and CBV 740 (Si/Al = 20) zeolites were prepared from NaY as reported previously.[27] Coumarin 6 was purchased from Aldrich and was recrystallized from ethanol prior to use. In its solid form, coumarin 6 is orange, but upon dissolving it in solvents such as $CH_2Cl_2$ or diglyme, the solution becomes yellow. Incorporation of coumarin 6 within the zeolite voids was accomplished by stirring known amounts of the dye in $CH_2Cl_2$ and adding to this solution the zeolite that had been previously activated at 400 °C for at least 6 h. Upon addition of the zeolite the mixture immediately changed color for most of the zeolite samples studied, turning various intensities of orange-red, indicating interaction with acidic sites. This mixture was then stirred for 3 h and filtered, and the solid washed with fresh $CH_2Cl_2$.. The $CH_2Cl_2$ washings were analyzed to determine how much of the dye was included. Different loadings were used, from 0.02 to 10 mg of coumarin 6 per gram of NaY. The dye included zeolites were then dried under reduced pressure (20−30 mTorr).

The zeolite NaY was saturated with pyridine by placing the activated zeolite in an uncapped vial which in turn was placed in a closed container of pyridine. The zeolite sample was left exposed to the pyridine vapor for a period of a few hours. The amount of pyridine included in the zeolite was determined by the resulting change in weight. This technique is the same employed in earlier work.[28]

Absorption of coumarin 6 on the BASF silica gel surface was achieved through stirring the dye and the silica gel in a dichloromethane solution for 3 h, followed by removal of solvent in vacuum and drying under a stream of dry $N_2$.

The montmorillonite clays SWy-1, STx-1, and Syn-1 were used without further purification as obtained from the Clay Minerals Society of the University of Missouri.

Coumarin 6 was incorporated into the clays by stirring about 3 g of clay in 150 mL of a solution of 10−100 mg/L of coumarin 6 in $CH_2Cl_2$. As in the case of zeolites, an instantaneous color change to orange-red from whitish-gray was also observed. The clay complexes were collected by suction filtration, followed by several washings with $CH_2Cl_2$ until the filtrate was colorless. The samples were then dried under vacuum for several hours before being analyzed. Reaction of the dye and the clays was also achieved in the solid state by grinding about 10 mg of coumarin 6 with ∼2 g of clay with a mortar and pestle. A color change, which was not as pronounced as that observed by solvent incorporation, was also noted.

Acidification of the clays was achieved using two different methods. One method involved washing the clay with a 4 N solution of sulfuric acid, while the other involved exchanging the cation sites with ammonium ions, followed by heating the clay at temperatures above 400 °C to drive off the resulting $NH_3$ that is produced. Exchanging the cation sites with $NH_4^+$ was accomplished by stirring the clay together with a 1 M solution of $NH_4Cl$, followed by suction filtration. This procedure was repeated twice to ensure that all or nearly all of the cation sites were in fact replaced with $NH_4^+$. It should be noted that this procedure resulted in some deterioration of the crystalline structure as determined by powder X-ray diffraction. The technique of pyridine exposure is similar to that described for the zeolite samples.

UV−vis absorption spectra were recorded on a Shimadzu 2101 PC using a $BaSO_4$ standard for the solid samples, and a Cary 1E spectrophotometer was used for the solution measurements. Fluorescence spectra were recorded on a Perkin-Elmer LS-50 spectrofluorimeter using a front face attachment for solid samples and for very concentrated solutions ($>1 \times 10^{-3}$ M) in dichloromethane. IR spectra of the dye included zeolites were recorded on a Nicolet 710 FTIR spectrometer using self-supported wafers (10 mg).

$^1$H NMR spectra of the free base and of the hydrochloride salt were recorded on a Bruker AMX 500 in $CDCl_3$. All chemical shifts were referenced to residual $CHCl_3$ and are reported relative to TMS = 0.00 ppm. 2D COSY NMR experiments were also recorded and are given in the Supporting Information.

Time-resolved fluorescence measurements were carried out using a Hamamatsu C-4334 streakscope coupled with a spectrograph capable of simultaneous spectral and time-resolved data acquisition. For the excitation source, the third harmonic from a continuum PY-61 picosecond Nd:YAG laser (355 nm, 35 ps, <4 mJ/pulse) was used. The kinetic data were fitted with either mono- or biexponential functions using the Hamamatsu software.

## Results

**Properties of Coumarin 6 in Solution.** Surprisingly, we could not find any previous reports on the acid−base properties of coumarin 6 in solution. We used techniques such as NMR, absorption, and fluorescence spectroscopy to gain some insight into the properties in organic solvents of this widely used laser dye. The absorption spectra of coumarin 6 in its neutral and protonated forms in $CH_2Cl_2$ are presented in Figure 1. The absorption $\lambda_{max}$ of the neutral form of the dye is at 450 nm in

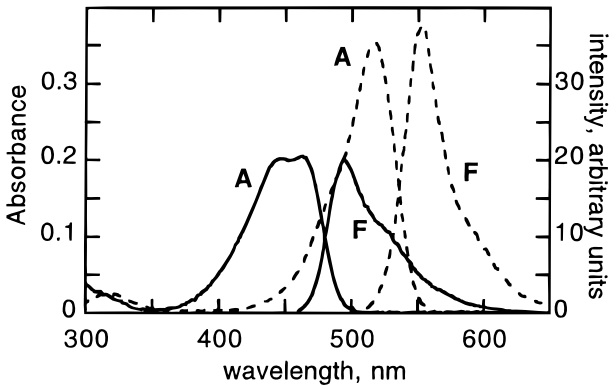


**Figure 1.** Absorption (A, left scale) and fluorescence (F, right scale) spectra of $4 \times 10^{-6}$ M coumarin 6 in $CH_2Cl_2$ for the neutral species (solid line) and for the monocation formed upon small addition of acid (dashed line).

**TABLE 1: $^1$H Chemical Shifts of the Neutral Compound and the HCl Salt of Coumarin 6[a]**

| | chemical shift, ppm | | |
|---|---|---|---|
| proton | neutral compd | HCl salt | $\delta\Delta$ |
| a | 1.24 | 1.27 | 0.03 |
| b | 3.45 | 3.51 | 0.06 |
| c | 6.55 | 6.53 | −0.02 |
| d | 6.65 | 6.70 | 0.05 |
| e | 7.47 | 7.91 | 0.44 |
| f | 8.90 | 10.02 | 1.12 |
| g | 7.95 or 8.02 | 7.70 | −0.25 or −0.32 |
| h | 7.35 or 7.48 | 7.50 | 0.15 or 0.02 |
| i | 7.48 or 7.35 | 7.60 | 0.12 or 0.25 |
| j | 8.02 or 7.95 | 8.38 | 0.36 or 0.43 |

[a] Assignments were based using a combination of 1D and 2D NMR. The benzothiazole protons for the neutral compound could not be determined unambiguously, thus both possibilities are listed.

**SCHEME 1**

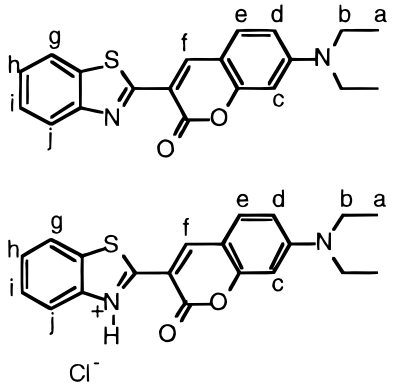


dichloromethane, and the $\lambda_{max}$ of the monocation is red-shifted and absorbs at 520 nm. The center of protonation for the monocation occurs exclusively at the ring nitrogen, as determined by $^1$H NMR spectroscopy. This was accomplished by comparing the peak positions of the free base form to that of the HCl salt dissolved in $CDCl_3$. The structures of both forms are shown in Scheme 1.

The assignments of the protons are straightforward using a combination of 1D and 2D NMR. These assignments are listed in Table 1. Although proton Hj could not be assigned unambiguously, the chemical shifts of 0.36−0.43 ppm indicate that this proton is affected by the decreasing electron density of the ortho nitrogen. Proton Hf undergoes a very large chemical shift upon protonation, as does proton He, though not to the same extent as Hf. The change in chemical shift for proton He can be rationalized in terms of resonance contributions, which is illustrated in Scheme 2.

**TABLE 2: Absorption and Fluorescence $\lambda_{max}$ of Coumarin 6 in Solution and the Solid State**

| system | abs $\lambda_{max}$ (nm) | fluor $\lambda_{max}$ (nm) |
|---|---|---|
| $CH_2Cl_2$ | 450 (neutral)<br>520 (monocation)<br>375 (dication) | 500<br>560 |
| 50% MeOH | 468 (neutral)<br>519 (monocation)<br>384 (dication) | 510<br>555<br>460 |
| $AlCl_3$ in trichlorobenzene | 520 | 535 |
| solid coumarin 6 | 460 (br)<br>570 (sh) | 630<br>630 |
| coumarin 6/HCl salt | 350 (br)<br>525 (br) | 485, 535<br>570, 700 |

**SCHEME 2**

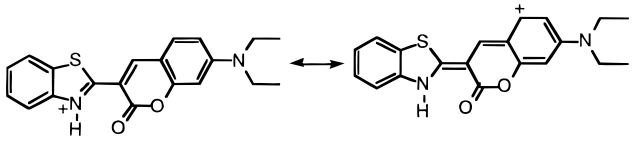


In contrast to the large changes in chemical shifts shown for protons e and f, protons b, c, and d exhibit negligible changes. This proves that the monocation formed is protonated exclusively at the ring nitrogen and not at the amino nitrogen.

The fluorescence spectra for the neutral and protonated forms are also shown in Figure 1 and have been normalized against the absorption spectra. The fluorescence spectra also show a relatively large shift in its $\lambda_{max}$ upon protonation, with a difference of 60 nm. The monocation species has a higher extinction coefficient compared to the neutral form, as is seen in Figure 1. The large red shift that occurs for coumarin 6 in both the UV−vis and fluorescence spectra upon formation of the monocation is attributed to the charge-transfer interaction that occurs from the electron-rich diethylamino moiety to the ring protonated benzothiazole. Additional amounts of acid result in formation of the dication species, with an absorption at 384 nm in 50% methanol, which is blue-shifted compared to the neutral species. The shifts in the absorption and fluorescence $\lambda_{max}$ in different solvents (see Table 2) are attributed to the change in the dipole moment of coumarin 6 due to the charge-transfer interactions. The change in the dipole moment between the ground and excited state was calculated through the use of the Lippert equation.[29] From a plot of the Stokes shift in various solvents against the polarizability function, $\Delta f$, of the solvent, the change in the dipole moment was calculated at 12 D. A gas-phase AM1 study[30] on the dipole moment of coumarin 6 in its ground and excited singlet state calculated the change in dipole moment to be only 1.6 D. Gas-phase calculations do not account for the occurrence of charge-transfer interactions, as is the case for coumarin 6. This accounts for the large difference that is seen between the measured and calculated values.

The p$K_a$ for the neutral to monocation equilibrium was measured through absorption spectroscopy using buffered solutions of the dye at different pH's. Due to the low solubility of coumarin 6 in water, the buffer solutions were prepared in 50/50 water/methanol and the dye was used in 0.2 vol % diglyme. A value of 1.6 was measured for the p$K_a$. This value was not corrected for the presence of the organic solvent.

When a Lewis acid such as $AlCl_3$ is added to a solution of coumarin 6 in trichlorobenzene, the resulting absorption spec-

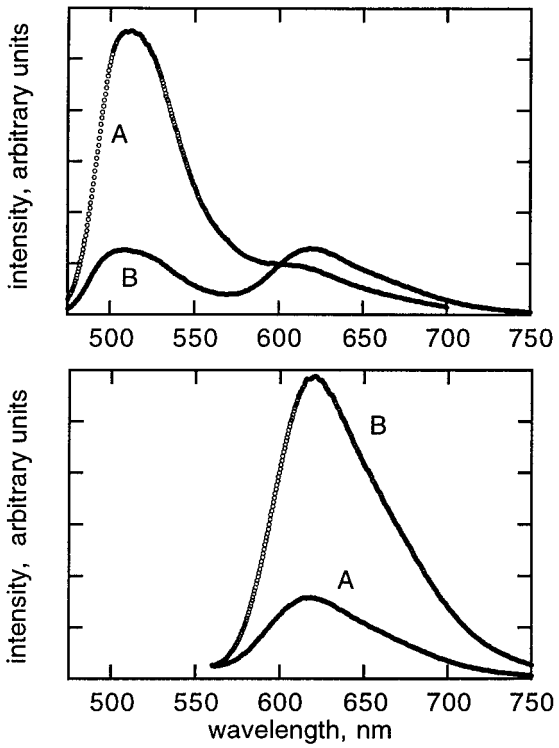


**Figure 2.** Fluorescence spectra of coumarin 6 with a $\lambda_{ex}$ of 450 nm (top) and a $\lambda_{ex}$ of 530 nm (bottom): (A) 0.0016 M of coumarin 6 in dichloromethane, (B) 0.016 M in dichloromethane. Note the decrease in intensity of the 620 nm band as the concentration decreases.

trum shows a $\lambda_{max}$ at 520 nm, which corresponds to the absorption of the monocation species. This shows that coumarin 6 is also sensitive to the presence of Lewis acids, forming a complex with them. The interaction of coumarin 6 with Brønsted and Lewis sites can be distinguished through use of IR spectroscopy. The frequency of the carbonyl stretching vibration changes from 1710 $cm^{-1}$ (neutral species) to 1650 $cm^{-1}$ (interaction with Lewis sites) to a broad band at 1689 $cm^{-1}$ with a shoulder at 1740 $cm^{-1}$ (Brønsted sites). All of these spectroscopic changes that coumarin 6 undergoes in solution in its neutral and protonated forms were used as a reference for the heterogeneous systems under study.

**Coumarin 6 in the Solid State.** Coumarin 6, a bright orange solid, and its hydrochloride salt, a purple solid, were studied using absorption and fluorescence spectroscopy. Both of these solids show a very large Stokes shift, which is on the order of 180 nm as well as significant band broadening when compared to solution spectra. The $\lambda_{max}$ values are listed in Table 2. Concentrated solutions of coumarin 6, which is also deep orange ($1.6 \times 10^{-2}$ M in dichloromethane), show an absorption in the 550 nm region in addition to its neutral form at 450 nm, as well as an additional emission band at 620 nm. The fluorescence spectra for concentrated solutions of coumarin 6 are shown in Figure 2. The 620 nm band becomes blue-shifted as the concentration of the dye decreases and eventually disappears at low dye concentrations ($<1.6 \times 10^{-4}$ M, yellow solution) along with the absorption at 550 nm. These results suggest some type of aggregation of the dye molecules. Time-resolved fluorescence measurements show that the emission from solid coumarin 6 is monoexponential, with a lifetime of 5.9 ns ($\lambda_{max}$ 630 nm). The HCl salt showed two components, with lifetimes of 199 ps and 1.1 ns ($\lambda_{max}$ 713 nm).

**Coumarin 6 Included within Zeolites.** The amount of coumarin 6 included within the faujasite zeolites NaY, HY21 (21% of the Na has been replaced by H), HY100 (Na fully exchanged by H), CBV 720 (Si/Al = 15), and CBV 740 (Si/Al = 20) was varied from very low loadings (0.02 mg of coumarin 6/g of zeolite) to high loadings (10 mg of coumarin 6/g of zeolite). This was done in order to determine the effect of dye concentration within the voids of the spherical supercages. As can be seen from Table 3, there is a significant red shift in the $\lambda_{max}$ of fluorescence in going from the lower loadings to the higher loadings of coumarin 6. This red shift is as large as 70 nm in the case of HY100. The $\lambda_{max}$ for absorption and fluorescence in the lower loading samples corresponds very well to those obtained in solution, whereas for the very high loadings, the values reported indicate that interactions other than acid−base are dominating the spectra. Figure 3 shows the change in the emission spectra of coumarin 6 included into NaY as the loading is increased.

**TABLE 3: Absorption and Fluorescence Maxima of Coumarin 6 in Zeolites and Clays[a]**

| system | loading, mg guest/ g host | absorp $\lambda_{max}$, nm | fluor $\lambda_{max}$, nm | assignt |
|---|---|---|---|---|
| NaY satd with pyridine | 0.02 | 460 | 515 | n |
| NaY | 10 | 520 | 585 | a |
| | 2 | 520 | 575 | a |
| | 0.4 | 520 (br) | 550 | m |
| | | | ($\lambda_{ex}$ 450) 510, 553 | n + m |
| | 0.02 | 520(br) | 540 | m |
| | | | ($\lambda_{ex}$ 450) 500 (sh), 540 | n + m |
| HY 100 | 10 | 510 | 607 | a |
| | 0.4 | 370 | 440, 540 | d + m |
| | | 520 | 550 | m |
| | 0.02 | 350 | 440, 540 | d + m |
| | | 520 | 535 | m |
| HY 21 | 10 | 520 | 585 | a |
| | 0.4 | 520 (br) | 555 | m |
| | 0.02 | 520 | 540 | m |
| silica gel BASF | 0.03 | 520 (br) | 560 | m |
| CBV 720 | 10 | 505 | 600 | a |
| | 0.02 | 400 | ($\lambda_{ex}$ 450) 495 (br) | |
| | | 510 | 540 (w) | m |
| CBV 740 | 10 | 500 | 590 | a |
| | 0.02 | 370 | 450, 550 | d + m |
| | | 520 | 540 | m |
| KY | 10 | 530 | 565, 600 (br) | a |
| CsY | <0.4 | 460 | 505 | n |
| STx-1 satd with pyridine | | 445, 520 (sh) | | |
| acidified STx-1 | | 398, 532 | | |
| SWy-1 | | 530 | 595 (w) | |
| STx-1 | | 535 | 565 (w) | |
| Syn-1 | | 526 | 575 | |

[a] The values reported are for vacuum-dried (20 mTorr) samples. Unless stated otherwise, the excitation wavelength corresponds to the absorption $\lambda_{max}$. n = neutral form, m = monocation, d = dication, a = aggregate.

The presence of residual solvent in the supercages and its effect on the acid−base properties of coumarin 6 were also studied. This was accomplished by drying one set of the inclusion complexes under a stream of nitrogen and by drying the other set under reduced pressure (20−30 mTorr). Differences between the two sets of samples are very apparent as can be seen by the color change that takes place along with the changes in the absorption and fluorescence spectra, resulting in better spectral resolution. These changes were most pronounced for the HY100 and CBV 740 zeolite samples. Thus, the values reported in the tables are for the vacuum-dried samples.

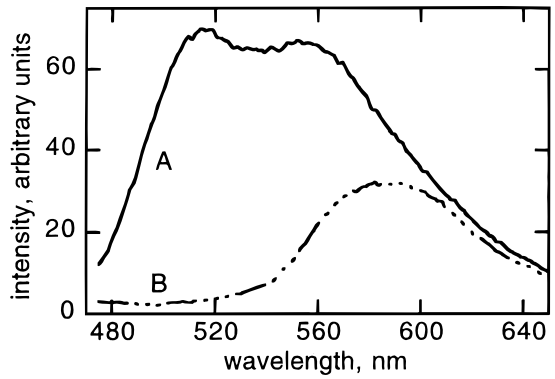


**Figure 3.** Fluorescence spectra of coumarin 6 included in NaY using an excitation wavelength of 450 nm: (A) 0.4 mg of coumarin 6/g of NaY; (B) 6 mg of coumarin 6/g of NaY. Note for the lower loading sample that emission from both the neutral and the monocation is observed.

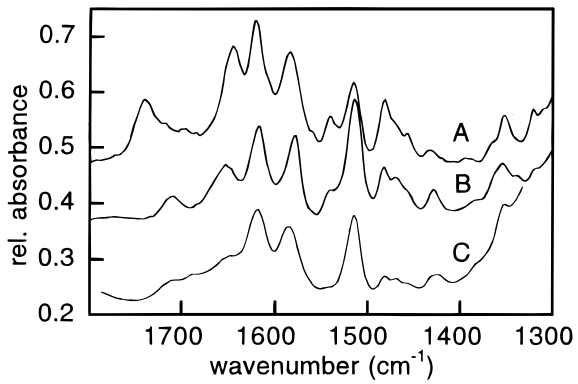


**Figure 4.** IR spectra of coumarin 6 included within the supercages of NaY, $\langle S \rangle = 0.04$ (plot A); KY, $\langle S \rangle = 0.04$ (plot B); and BASF silica gel (plot C). Note the strong band at 1517 $cm^{-1}$ present in all three samples, indicating a Lewis acid interaction with coumarin 6.

The faujasite zeolite NaY was treated with pyridine (corresponding to a pyridine occupancy of 1.5 molecules per supercage) followed by addition of coumarin 6. This addition did not cause an immediate change in color, as occurred for the other zeolites. The resulting absorption spectrum had a peak centered at 460 nm and an emission occurring at 515 nm. When a sample of coumarin 6 included in NaY (having the same loading as above) is exposed to pyridine vapors, the inclusion complex immediately begins to change color from red to yellow. The absorption spectra before and after pyridine exposure shows a shift in the $\lambda_{max}$ from 515 to 460 nm.

The alkali ion exchanged faujasite zeolite, CsY, was also used in the present study to determine the effect that changing the counterion to a different alkali metal has on the spectra of coumarin 6. CsY was the only zeolite in the present study that did not change the color of the coumarin 6 dichloromethane solution upon its addition. The absorption spectrum of the dye included in CsY had a $\lambda_{max}$ at 460 nm. This absorption spectrum correlates very well with the neutral species of the dye. The fluorescence $\lambda_{max}$ of this sample is at 504 nm. A summary of the absorption and fluorescence $\lambda_{max}$ for coumarin 6 in various heterogeneous systems is presented in Table 3.

The IR spectra of the higher loading of the dye incorporated in the alkali exchanged faujasites NaY and KY were also recorded. These spectra, along with that obtained by adsorption of coumarin 6 onto silica gel, are shown in Figure 4. The intense carbonyl stretching frequency which appears at 1710 $cm^{-1}$ for the neutral dye is very weak in these samples. There are very strong bands that appear at 1645 and 1653 $cm^{-1}$ for the NaY and KY samples, respectively, and all three samples show a very strong band at 1517 $cm^{-1}$, indicative of a Lewis acid interaction with coumarin 6.

**Coumarin 6 Included within Clays and Silica Gel.** In addition to zeolites, the dye was incorporated into three different clays: Swy-1, a Na−montmorillonite clay; STx-1, a Ca−montmorillonite clay; and Syn-1, a synthetic mica−montmorillonite clay. Dye incorporation must initiate on the exterior surface, although the swelling solvents used may cause some interlayer inclusion. Surprisingly, incorporation of the dye using two different methods, one of stirring a suspension of the clay and coumarin 6 in dichloromethane and the second by grinding the clay and dye together, produced the same qualitative results: the absorption $\lambda_{max}$ for all the clays occurs at 530 nm. The clays were also acidified by replacing the cation exchange sites with protons, followed by incorporation of the dye molecule. This resulted in an absorption spectrum of the acidified STx-1/coumarin 6 sample having a $\lambda_{max}$ at 400 nm and a more intense peak at 532 nm. Absorption at 400 nm corresponds to the dicationic species of the dye that is observed in solution. The STx-1 clay was also exposed to pyridine vapor, followed by incorporation of the dye, which resulted in an absorption spectrum corresponding mainly to the neutral species of coumarin 6, with some monocationic species present. The UV−vis absorption and fluorescence maxima obtained for the dye included clay samples are also listed in Table 3, when available. The high levels of iron present in some of the clay samples (e.g., STx-1) resulted in extensive quenching of the fluorescence signal.

A few exploratory experiments were also carried out in silica gel, using the same incorporation procedure as with the clays. The spectra revealed the formation of the protonated form of coumarin 6.

## Discussion

Coumarin 6 incorporated into heterogeneous systems is able to detect weak acid sites that are present in the host system. The similarity of the changes seen in its absorption spectrum upon addition of a Lewis acid or Brønsted acid in solution reveals that this dye can detect both types of acidity very effectively. The amount of dye included is very important, as too large a loading causes a significant red shift in the $\lambda_{max}$ when compared to solution values. This red shift is attributed to the formation of aggregates of the dye, which is seen in both concentrated solutions of coumarin 6 as well as the solid state. The absorption band that is attributed to aggregate formation is red-shifted compared to the monomer and is thus ascribed to a head-to-tail or J-aggregate. Since high concentrations of the dye ($>10^{-3}$ M) are required in order to detect any aggregates, we believe that the equilibrium constant in dichloromethane must be very low, on the order of $10^{1}$ M.

At the small dye loadings used in this study, the probability of aggregate formation is extremely low compared to the interactions of coumarin 6 with acidic sites in the zeolite. The dye, being a base, must have a preference for the more acidic sites, just as pyridine does.[28] Hence, the formation of the monocation or the dication of the dye can be properly assigned. The relative amount of Lewis or Brønsted sites for a given loading can be determined based on the species of the dye that is detected upon inclusion. In the series of zeolites NaY, HY21, and HY100, the incorporation of coumarin 6 yielded some interesting results. In the case of NaY, the absorption and fluorescence spectra reveal that the majority of the dye is present as the monocation. Some of the neutral form was also detected,

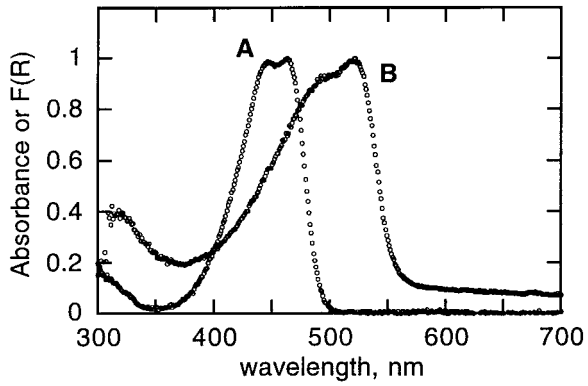


**Figure 5.** Normalized absorption or reflectance function [$F(R)$] spectra of coumarin 6. Curve A is the absorption spectrum in dichloromethane, and curve B is the Kubelka−Munk function spectrum in NaY.

as indicated by the peak at 510 nm in the emission spectrum with excitation at 450 nm. A comparison of the absorption of coumarin 6 in dichloromethane and in NaY is presented in Figure 5. This clearly shows that in NaY, which has been considered as a nonacidic zeolite, that there are enough acidic sites such as to alter the photophysical properties of included organics. We have shown this in an earlier report whereby the triplet lifetime of xanthone in NaY was altered dramatically in the presence of pyridine, which is able to quench the acid sites.[28] In the case of HY 21, only the monocation species was detected, whereas for HY 100, both the monocation and the dication were detected.

Unlike the series NaY, HY 21, and HY 100, which increases in Brønsted acidity, the series NaY, CBV 720, and CBV 740 was chosen because of the increase in Lewis acidity caused by the increase in the acidity of the remaining acid sites. For the CBV 720 zeolite, the emissions from both the neutral form and the monocation were detected. On the other hand, no neutral species was detected in CBV 740, but there is evidence for the formation of both the monocation and dication. In all of the zeolites studied, the dication of coumarin 6 was detected in only HY100 and CBV 740, which are the most acidic Brønsted and Lewis zeolites, respectively, used in the present study.

The saturation of NaY with pyridine was done in order to quench all of the acid sites present. Inclusion of coumarin 6 into a pyridine-saturated NaY zeolite resulted in only the neutral form of the dye, unlike a pyridine-free sample in which the majority of the dye is in its monocation form. The shift in the absorption $\lambda_{max}$ that is seen for the coumarin 6 included in NaY as it becomes exposed to pyridine vapors indicates that pyridine is quenching the acid sites, causing the dye to change from its monocation form to the neutral form. This is also confirmed by the fluorescence spectra.

The series of faujasites, NaY and CsY, were used because of the known increase in basicity of the zeolite going down in the periodic table. As mentioned above, coumarin 6 was able to detect acidity in the NaY zeolite, although none was detected for the more basic CsY zeolite. Only a small amount of organic could be included within CsY compared to the other zeolites used in this series, due to size restraints. The IR spectrum of the dye included within NaY confirms that the acidity of these zeolites is due to the presence of Lewis sites, with the characteristic band at 1650 $cm^{-1}$ (interaction of carbonyl with Lewis acid). In both of these cases, the neutral form of the dye is still detected, thereby indicating a mixture of both interacting and noninteracting coumarin 6 within the zeolite. No bands due to the presence of Bronsted acids were observed in the IR spectra. Though NaY is not a strongly acidic zeolite, the acid−base interaction with coumarin 6 and the counterions present within these zeolites does explain the absorbance and fluorescence changes seen in these systems.

Coumarin 6 is also fairly insensitive to the presence of water, since in 50/50 solution of acetonitrile/$H_2O$, it does not undergo significant changes in its absorption or fluorescence spectra with respect to pure acetonitrile. The insensitivity of coumarin 6 to the presence of water, unlike other dye molecules such as methylene blue[31] which shifts by 70 nm going from a hydrated to a dehydrated faujasite zeolite, makes the use of this coumarin in the study of zeolite systems even more attractive. Zeolites are very hygroscopic materials that must be activated prior to use and handled in such a way as to minimize the amount of moisture that is reabsorbed. Thus, the use of coumarin 6 in different zeolite systems that may vary slightly in water content due to handling differences will not affect the outcome of the absorption or fluorescence spectra. This is not the case when using pyridine as a probe molecule, as this molecule is extremely sensitive to the presence of absorbed water in faujasite zeolites. This has been previously detected using FT-Raman spectroscopy.[12]

The diffuse reflectance and fluorescence spectra of coumarin 6 interacting with BASF silica gel reveal the presence of the monocation species of coumarin 6. The BASF sample used did not show any cracking activity at 300 °C and has been used as a standard for zero acidity in such tests. The detection of the monocation form of coumarin 6 in this sample once again shows the remarkable sensitivity of the dye to very weakly acidic silanol groups. The fluorescence spectra for the BASF sample using a $\lambda_{ex}$ corresponding to neutral and monocation species both give rise to a $\lambda_{max}$ at 560 nm, indicative of monocation fluorescence. From the IR spectrum (Figure 4) the interaction of coumarin 6 with the silanol groups is based on complexation rather than proton transfer. The possibility of coumarin 6 undergoing excited-state proton transfer was taken into account since these types of molecules are known to become stronger bases in the excited state. Using both time-resolved and steady-state fluorescence measurements, no indication of this process occurring was seen either in solution or in the silica gel BASF sample.

## Conclusions

We have presented the acid−base properties of coumarin 6 in solution as well as the spectroscopic properties of both the solid and the hydrochloride salt. This molecule has a large amount of CT character, and as a result the difference in dipole moment between the ground and excited state is fairly large, being measured at 12 D. The center of protonation occurs at the ring nitrogen, proven using a combination of 1D and 2D NMR of free base and hydrochloride salt. In the solid state and in concentrated solutions, coumarin 6 has been found to form aggregates. In heterogeneous systems, this dye shows remarkable sensitivity for detecting acidity in the faujasite zeolite NaY as well as for silica gel BASF, which is used as a standard for zero acidity. The dication was formed in HY 100 and CBV 740 which are the most highly Brønsted and Lewis acidic zeolites, respectively, used in this study. The sensitivity of coumarin 6 to its microenvironment as well as the large spectral shifts between the neutral, monocation, and dication forms makes it a good candidate for studying other heterogeneous systems as well.

**Acknowledgment.** Financial support by the Natural Science and Engineering Council of Canada through a Research Grant

(J.C.S.) and a graduate scholarship (S.C.) and Spanish DGICYT (H.G., Project # PB93-0380) are gratefully acknowledged. Thanks are due to G. Cosa for assistance with the picosecond measurements.

**Supporting Information Available:** 2D COSY NMR spectra of coumarin 6 and its protonated form (2 pages). Ordering information is given on any current masthead page.

## References and Notes

(1) Breck, D. W. *Zeolite Molecular Sieves: Structure, Chemistry and Use*; Wiley and Sons: New York, 1974.
(2) Townsend, R. P. *Introduction to Zeolite Science and Practice*; Elsevier: Amsterdam, 1991; Vol. 58.
(3) Corma, A.; Fornés, V.; Rey, F. *Appl. Catal.* **1990**, *59*, 267.
(4) Marshall, K.; Ridgewell, G. L.; Rochester, C. H.; Simpson, J. *Chem. Ind.* **1974**, *5*, 775.
(5) Farneth, W. E.; Gorte, R. J. *Chem. Rev.* **1995**, *95*, 615.
(6) Corma, A. *Chem. Rev.* **1995**, *95*, 559.
(7) Guimon, C.; Zouiten, A.; Boreave, A.; Pfister-Guillouzo, G. *J. Chem. Soc., Faraday Trans.* **1994**, *90*, 3461.
(8) Karge, H. G.; Dondur, V.; Weitkamp, J. *J. Phys. Chem.* **1991**, *95*, 283.
(9) Katada, N.; Igi, H.; Kim, J.-H.; Niwa, M. *J. Phys. Chem. B* **1997**, *101*, 5969.
(10) Ferwerda, R.; van der Maas, J. H.; Hendra, P. J. *Vib. Spectrosc.* **1994**, *7*, 37.
(11) Egerton, T. A.; Hardin, A. H.; Sheppard, N. *Can. J. Chem.* **1976**, *54*, 586.
(12) Ferwerda, R.; van der Maas, J. H.; Hendra, P. J. *J. Phys. Chem.* **1993**, *97*, 7331.
(13) Ferwerda, R.; van der Maas, J. H. *J. Phys. Chem.* **1995**, *99*, 14764.
(14) Haw, J. F.; Nicholas, J. B.; Xu, T.; Beck, L. W.; Ferguson, D. B. *Acc. Chem. Res.* **1996**, *29*, 259.
(15) Gil, B.; Broclawik, E.; Datka, J.; Klinowski, J. *J. Phys. Chem.* **1994**, *98*, 930.
(16) Drago, R. S.; Dias, S. C.; Torrealba, M.; de Lima, L. *J. Am. Chem. Soc.* **1997**, *119*, 4444.
(17) Place, R. D.; Dutta, P. K. *Anal. Chem.* **1991**, *63*, 348.
(18) Abdel-Mottaleb, M. S. A.; Loutfy, R. O.; Lapouyade, R. *J. Photochem. Photobiol. A: Chem.* **1989**, *48*, 87.
(19) Abdel-Mottaleb, M. S. A.; Antonious, M. S.; Abo Ali, M. M.; Ismail, L. F. M.; El-Sayed, B. A.; Sherief, A. M. K. *Proc. Indian Acad. Sci.* **1992**, *104*, 185.
(20) Jones, G. I.; Jackson, W. R.; Choi, C. *J. Phys. Chem.* **1985**, *89*, 294.
(21) Odom, I. E. *Philos. Trans. R. Soc. London A* **1984**, *311*, 391.
(22) Billingham, J.; Breen, C.; Yarwood, J. *Clay Miner.* **1996**, *31*, 513.
(23) del Rey-Bueno, F.; García-Rodríguez, A.; Mata-Arjona, A.; del Rey-Pérez-Caballero, F. J. *Clays Clay Miner.* **1995**, *43*, 554.
(24) Zubkov, S. A.; Kustov, L. M.; Kazansky, V. B.; Fetter, G.; Tichit, D.; Figueras, F. *Clays Clay Miner.* **1994**, *42*, 421.
(25) Kumar, P.; Jasra, R. V.; Bhat, T. S. G. *Ind. Eng. Chem. Res.* **1995**, *34*, 1440.
(26) Corma, A.; García, H.; Iborra, S.; Primo, J. *J. Catal.* **1989**, *120*, 78.
(27) Beyer, H. K.; Belenkaya, I. *Catalysis by Zeolites*; Elsevier: Amsterdam, 1980.
(28) Scaiano, J. C.; Kaila, M.; Corrent, S. *J. Phys. Chem. B* **1997**, *101*, 8564.
(29) Lippert, E. *Z. Naturforsch.* **1955**, *A10*, 541.
(30) McCarthy, P. K.; Blanchard, G. J. *J. Phys. Chem.* **1993**, *97*, 12205.
(31) Ehrl, M.; Kinervater, H. W.; Deeg, F. W.; Bräuchle, C. *J. Phys. Chem.* **1994**, *98*, 11756.